

CHAPTER 156

Swash Dynamics under Obliquely Incident Waves

Nobuhisa Kobayashi¹, and Entin A. Karjadi²

ABSTRACT: A horizontally two-dimensional, numerical model is developed for predicting the time-dependent free surface elevation and fluid velocities in the swash and surf zones under obliquely incident waves. The assumptions of shallow water waves with small incident angles are made to simplify the continuity and momentum equations and reduce computational efforts considerably. The developed numerical model allows gradual alongshore variations of the bathymetry and the incident regular or irregular waves at its seaward boundary. The numerical model is compared with available regular wave data of alongshore uniformity as an initial assessment of the model. The wave height, setup and runup are predicted well. The numerical model with the bottom friction factor calibrated previously for swash oscillations predicts the magnitude of longshore current but can not reproduce the longshore current profile probably because it does not model the transition zone and lateral mixing.

INTRODUCTION

A quantitative understanding of swash hydrodynamics and sediment transport on beaches under obliquely incident waves is essential for the design of shoreline erosion mitigation measures such as sand bypassing and beach nourishment. Field and laboratory measurements on the distribution of longshore sediment transport across the surf zone indicated that the distribution was generally bimodal with peaks in the swash and breaker zones (e.g., Bodge and Dean 1987; Kamphuis 1991). Bodge and Dean (1987) observed that the relative significance of the peaks shifted from the breaker zone peak to the swash zone peak as the surf varied from spilling to collapsing conditions. They found that longshore sediment transport in the swash zone might account for at least 5% to over 60% of the total drift. Knowledge of longshore sediment transport in the swash zone is important for the design of a sand bypassing system such as the system based on a jet pump deployed in the swash zone at Indian River Inlet, Delaware (Clausner et al. 1991).

Ryrie (1983) developed a time-dependent numerical model for longshore fluid motion along a straight shoreline with a plane slope generated by obliquely incident monochromatic waves with a small angle of incidence. The numerical model was not compared with any data. The numerical model developed herein is formulated

¹Prof., Dept. of Civ. Eng., and Assoc. Dir., Ctr. for Applied Coast. Res., Univ. of Delaware, Newark, DE 19716, USA.

²Ph.D. Student, Ctr. for Applied Coast. Res., Univ. of Delaware, Newark, DE 19716, USA.

unlike that of Ryrie (1983) such that it will be applicable to beaches of arbitrary geometry under obliquely incident random waves. Approximate two-dimensional governing equations under the assumptions of shallow water waves with small angles of incidence are derived from the three-dimensional continuity and Reynolds equations (e.g., Rodi 1980) in a manner similar to the derivation of Kobayashi and Wurjanto (1992) of approximate one dimensional equations from the two-dimensional continuity and Reynolds equations. It should be noted that the mechanical energy equation for turbulent flow can be derived from the continuity and Reynolds equations and that the energy equation for turbulent flow is generally associated with the conservation of heat energy (e.g., Rodi 1980).

TIME-DEPENDENT NUMERICAL MODEL

The cartesian coordinate system (x', y', z') is defined as x' = horizontal coordinate normal to the overall orientation of the shoreline; y' = horizontal coordinate normal to the x' -axis; and z' = vertical coordinate with $z' = 0$ at the still water level (SWL). The prime indicates the physical variables that will be normalized later. Limiting to waves in shallow water, the coordinates x' , y' and z' are normalized by $\sigma H'$, $\sigma H'/\theta_c$ and H' , respectively, where H' = incident wave height; θ_c = reference incident wave angle in radian; and $\sigma = T'\sqrt{g/H'}$ with T' = incident wave period and g = gravitational acceleration. The corresponding fluid velocity components u' , v' and w' in the x' , y' and z' directions are normalized by $\sqrt{gH'}$, $\theta_c\sqrt{gH'}$ and H'/T' , respectively. The normalized continuity and Reynolds equations are then simplified under the assumptions of $\sigma^2 \gg 1$ and $\theta_c^2 \ll 1$ for shallow water waves with small angles of incidence. The simplified equations are integrated from the bottom to the instantaneous free surface using the kinematic bottom and free surface boundary conditions as well as the boundary conditions of zero normal and tangential stresses at the free surface.

The derived continuity and horizontal momentum equations for $\sigma^2 \gg 1$ and $\theta_c^2 \ll 1$ are expressed in the following normalized forms (Kobayashi and Karjadi 1995)

$$\frac{\partial h}{\partial t} + \frac{\partial}{\partial x}(hU) = 0 \quad (1)$$

$$\frac{\partial}{\partial t}(hU) + \frac{\partial}{\partial x}(C_1 hU^2) = -h \frac{\partial \eta}{\partial x} - f|U|U \quad (2)$$

$$\frac{\partial}{\partial t}(hV) + \frac{\partial}{\partial x}(C_2 hUV) = -h \frac{\partial \eta}{\partial y} - f|U|V \quad (3)$$

The normalized variables without the prime in these equations are defined as

$$t = \frac{t'}{T'} ; x = \frac{x'}{\sigma H'} ; y = \frac{y'}{\sigma H'/\theta_c} ; h = \frac{h'}{H'} ; \eta = \frac{\eta'}{H'} \quad (4)$$

$$U = \frac{U'}{\sqrt{gH'}} ; V = \frac{V'}{\theta_c \sqrt{gH'}} ; f = \frac{1}{2} \sigma f' ; \sigma = \frac{T'\sqrt{gH'}}{H'} \quad (5)$$

where t = time; h = instantaneous water depth; η = instantaneous free surface elevation above SWL; U = depth-averaged value of the cross-shore velocity u ; V = depth-averaged value of the longshore velocity v ; f' = bottom friction factor used to express the bottom shear stress in terms of U and V ; and σ = ratio between the

cross-shore and vertical length scales. The momentum correction coefficients C_1 and C_2 equal the depth-averaged values of $(u/U)^2$ and (uv/UV) , respectively. It is noted that the vertical momentum equation yields essentially hydrostatic pressure in shallow water. Eqs. (1) and (2) with $C_1 = 1$ are the same as those used previously for predicting the setup and runup of normally incident waves (Kobayashi and Wurjanto 1992). The assumption of $C_1 = 1$ was suggested to result in an error on the order of 10%. The assumption of $C_2 = 1$ in (3) may also be made to compute V using (3) for the temporal and spatial variations of U and h computed using (1) and (2). For the case of $\theta_c^2 \ll 1$, the dominant cross-shore fluid motion is not affected by the secondary longshore fluid motion varying more slowly in the longshore direction. Furthermore, the variations in the y -direction appear only in the term $\partial\eta/\partial y$ in (3) and along the seaward boundary of the computation domain. The alongshore momentum equation (3) is more sensitive to the gradual alongshore variability. In short, the assumption of $\theta_c^2 \ll 1$ reduces computational efforts considerably and eliminates difficulties associated with lateral boundary conditions for general two-dimensional computations.

The instantaneous quantities h, U and V in (1)–(3) include both oscillatory and mean quantities. The time-averaged continuity equation corresponding to (1) yields $\overline{h\bar{U}} = 0$ to satisfy the condition of no flux into the assumed impermeable beach where the overbar denotes time averaging. The time-averaged momentum equation corresponding to (2) with $C_1 = 1$ and $f = 0$ corresponds to the conventional cross-shore momentum equation used to compute wave setup $\bar{\eta}$ (Kobayashi et al. 1989). The time-averaged alongshore momentum equation corresponding to (3) with $C_2 = 1$ can be written as

$$\frac{\partial}{\partial x} S_{xy} = -f|U|\bar{V} - \bar{h} \frac{\partial \bar{\eta}}{\partial y} - \frac{1}{2} \frac{\partial}{\partial y} \left[\overline{(\eta - \bar{\eta})^2} \right] \quad (6)$$

with

$$S_{xy} = \overline{hUV} = \overline{hU(V - \bar{V})} \quad (7)$$

If the setup $\bar{\eta}$ and the variance $\overline{(\eta - \bar{\eta})^2}$ related to the root mean square wave height do not vary in the alongshore direction, (6) is similar to the conventional alongshore momentum equation that assumes $\bar{U} = 0$. The gradual alongshore variations of the wave setup and variance are as important as the bottom friction and the cross-shore gradient of the alongshore radiation stress S_{xy} for a small angle of wave incidence. The dispersion or lateral mixing term due to the vertical variations of u and v (e.g., Rodi 1980) is neglected in (6) because of the assumption of $C_2 = 1$ employed here. Svendsen and Putrevu (1994) discussed the vertical variations of the mean velocities \bar{u} and \bar{v} and attributed the lateral mixing due to the nonlinear interaction between \bar{u} and \bar{v} . The dispersion terms arise from the nonlinear interaction between $(u - U)$ and $(v - V)$ integrated over the depth in conventional turbulent flow analyses (e.g., Rodi 1980).

Fig. 1 shows the finite difference grid of constant grid sizes Δx and Δy used in the numerical model. The cross-shore coordinate x is taken to be positive landward and the alongshore coordinate y is positive in the downwave direction with $y = 0$ at the upwave boundary. The seaward boundary of the computation domain is located at $x = 0$ along the y -axis. The time step size Δt is allowed to vary in the same way

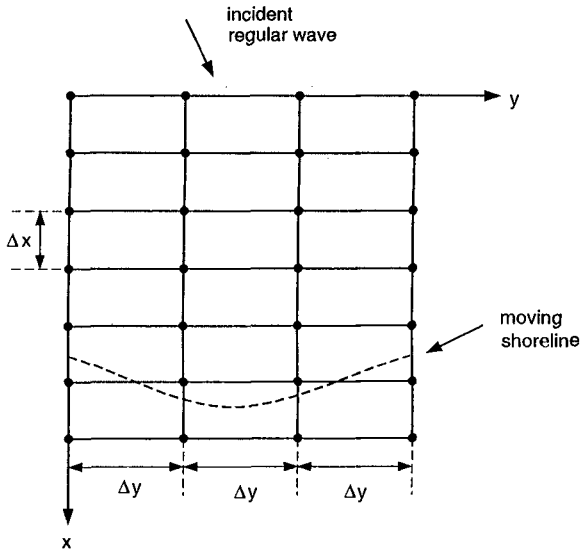


Figure 1: Finite Difference Grid for Numerical Model

as in the existing one-dimensional numerical model RBREAK2 (Kobayashi and Poff 1994) where Δt is reduced in a semiautomated manner whenever numerical difficulties occur at the moving shoreline. The initial time $t = 0$ for the computation marching forward in time is taken to be the time when the incident wave train arrives at $x = 0$ and there is no wave action in the region $x \geq 0$ and $y \geq 0$.

For the known values of h , η , $m = hU$ and $q = hV$ at the time level t , the values of these variables at the next time level $t^* = (t + \Delta t)$, which are denoted by the asterisk, are computed in sequence. The value of $(h - \eta)$ is the normalized depth below SWL which is known for the specified bottom elevation. First, along each of the shore-normal lines at $y = (i - 1)\Delta y$ with $i = 1, 2, \dots, I$ where I is the number of the shore-normal lines, h^* and m^* are computed by solving (1) and (2) using the explicit dissipative Lax-Wendroff method (e.g., Richtmyer and Morton 1967) together with the seaward and landward boundary conditions employed in RBREAK2 (Kobayashi et al. 1987, 1989). The obliquely incident wave train at the seaward boundary is specified as input. The computation along each shore-normal line is actually made using RBREAK2. Second, along each of the shore-normal lines at $y = (i - 1)\Delta y$ with $i = 2, 3, \dots, (I - 1)$, q^* is computed using (3) together with the computed h^* and m^* where $\partial\eta/\partial y$ in (3) is approximated by a central finite difference based on the values of η^* at the two adjacent lines. Use is made of the MacCormack method (MacCormack 1969) which is a simplified version of the Lax-Wendroff method and has been used successfully for the computation of unsteady open channel flows with hydraulic jumps (e.g., Gharangik and Chaudhry 1991). q^* is set zero landward of the shoreline node computed by RBREAK2. The seaward boundary condition for q^* is based on the characteristic equation derived from (3) as explained by Kobayashi and

Table 1: Incident Waves at Seaward Boundary $x' = 0$

Expt. No.	$\tan \theta'$	d'_i (cm)	T' (s)	H' (cm)	θ_i (deg)	σ	θ_c^2	ξ
2	0.101	21.1	1.00	9.5	26.0	10.2	0.206	0.409
3	0.101	21.3	1.00	8.7	14.2	10.6	0.061	0.428
4	0.050	18.5	1.02	7.9	13.9	11.4	0.059	0.227
5	0.050	18.2	1.85	9.0	12.9	19.3	0.051	0.385

Karjadi (1995).

When the beach profile and incident wave conditions are uniform in the longshore direction, it is sufficient to compute $h(t, x)$, $\eta(t, x)$ and $m(t, x) = h(t, x) U(t, x)$ along the three lines at $y = 0$, Δy and $2\Delta y$ and $q(t, x) = h(t, x) V(t, x)$ along the line at $y = \Delta y$. The computed η along the three lines are used to ensure the alongshore uniformity of the mean and variance of η used in (6). Even if the beach profile and incident wave conditions vary gradually alongshore, the developed numerical model will be applicable for the computation of the gradual longshore variations of h , m and q by choosing a larger value of I , provided that lateral boundary conditions do not affect h , m and q in the computation domain.

COMPARISON WITH AVAILABLE REGULAR WAVE DATA

Visser (1991) conducted eight monochromatic wave experiments on 1:10 and 1:20 slopes and presented detailed data on uniform longshore currents, local wave heights, angles of wave incidence, wave setup and runup. The numerical model is compared with four experiments for which the seaward boundary location can be taken to be in relatively shallow water seaward of the breaker line. Table 1 lists the experiment number used by Visser (1991) and the slope and incident wave characteristics specified as input to the numerical model where $\tan \theta' =$ uniform slope; $d'_i =$ water depth below SWL at the seaward boundary located at $x' = 0$; $T' =$ wave period; $H' =$ incident wave height at $x' = 0$; $\theta_i =$ angle in degrees of wave incidence at $x' = 0$; $\sigma =$ ratio between the cross-shore and vertical length scales defined in (5); $\theta_c =$ reference incident wave angle in radian taken to be θ_i in radian; and $\xi =$ surf similarity parameter given by $\xi = \sigma \tan \theta' / \sqrt{2\pi}$. For these experiments, plunging breakers were observed. The assumptions of $\sigma^2 \gg 1$ and $\theta_c^2 \ll 1$ may be appropriate except for Experiment 2 with $\theta_c^2 = 0.206$. The only empirical parameter involved in the numerical model is the bottom friction factor f' in (5) where $f' \simeq 0.05$ has been used for predicting wave runup on smooth slopes in small-scale experiments (e.g., Kobayashi et al. 1989). The value of $f' = 0.05$ is used here for both cross-shore and alongshore fluid motions.

The obliquely incident regular wave train $\eta'_i(t', y')$ at $x' = 0$ for the small angle θ_i in radian is assumed to be in the following dimensional form

$$\eta'_i(t', y') = \text{periodic function of } \left(\frac{t'}{T'} - \frac{y'}{L'/\theta_i} \right) = \frac{1}{T'} \left(t' - \frac{y'}{C'/\theta_i} \right) \quad (8)$$

in which L' and $C' = L'/T'$ are the wavelength and phase velocity in the water depth

d'_t . Eq. (8) accounts for the phase or time lag along the alongshore coordinate y' . The periodic function in (8) is specified using Stokes second-order or cnoidal wave theory depending on the value of Ursell parameter (Kobayashi et al. 1987).

The normalized grid sizes Δx and Δy in Fig. 1 need to be chosen to be small enough to resolve breaking waves in the surf and swash zones. For these experiments of alongshore uniformity, it is sufficient to use the three cross-shore lines at $y = 0$, Δ and $2\Delta y$ in Fig. 1. The value of Δx is selected to be on the order of 0.01, corresponding to 200 grid spacings between the seaward boundary and the still water shoreline. The value of Δy is chosen to be the same as Δx to yield the same spatial resolution in the normalized coordinates. A limited sensitivity analysis has indicated that the computed results remain essentially the same as long as Δy is on the order of Δx or less.

First, the detailed computed results for Experiment 2 are presented as an example. The temporal and cross-shore variations of the free surface elevation η , the depth-averaged cross-shore velocity U , and the depth-averaged alongshore velocity V are stored along the center line at $y = \Delta y$. The temporal variations of η , U and V for the duration $0 \leq t \leq 300$ at $x = 0$ (at the seaward boundary), $x = 0.509$ (immediately seaward of the breaker line), $x = 0.770$ (in the outer surf zone), $x = 1.550$ (in the inner surf zone), and $x = 2.265$ (in the swash zone) are shown in Figs. 2, 3 and 4, respectively. The cross-shore fluid motion represented by η and U computed using (1) and (2) becomes periodic fairly quickly for $t \gtrsim 20$ as has been the case with the previous one-dimensional computations for beaches (e.g., Kobayashi et al. 1989). The alongshore fluid motion represented by V computed using (3) becomes periodic very slowly especially in the vicinity of the breaker line. The very slow response of the alongshore fluid motion is qualitatively consistent with the analytical result of Ryrie (1983) for the periodic solution development as well as the experimental procedure adopted by Visser (1991) who made measurements one hour after the start of the wave maker. In light of Fig. 4, the time averaging denoted by the overbar in the following is performed for the duration $200 \leq t \leq 300$.

The computed cross-shore variations of $\bar{\eta}$, η_{rms} , \bar{U} , U_{rms} , \bar{V} and V_{rms} for Experiment 2 are shown in Fig. 5 where the root-mean-square values representing the magnitude of the oscillatory components are defined as

$$\eta_{rms}^2 = \overline{(\eta - \bar{\eta})^2} ; U_{rms}^2 = \overline{(U - \bar{U})^2} ; V_{rms}^2 = \overline{(V - \bar{V})^2} \quad (9)$$

For example, if $\eta = 0.5 \cos(2\pi t)$, $\bar{\eta} = 0$ and $\eta_{rms} = 1/\sqrt{8} = 0.35$. The normalized uniform slope is indicated by the dashed-dotted straight line in the top figure in Fig. 5. The upper limit of the wave setup $\bar{\eta}$ is the maximum runup elevation on the slope above SWL because $\bar{h} \geq 0$ in the region wetted by water. The increase of $\bar{\eta}$ and the decrease of η_{rms} in the surf and swash zone are approximately linear. On the other hand, U_{rms} decreases slowly in the surf zone and rapidly in the swash zone. \bar{U} is negative and represents the cross-shore return current as explained by Kobayashi et al. (1989). The longshore current \bar{V} is dominant in the surf zone and the oscillatory component V_{rms} decreases approximately linearly in the surf and swash zone.

Fig. 6 shows the computed cross-shore variations of the normalized quantities in-

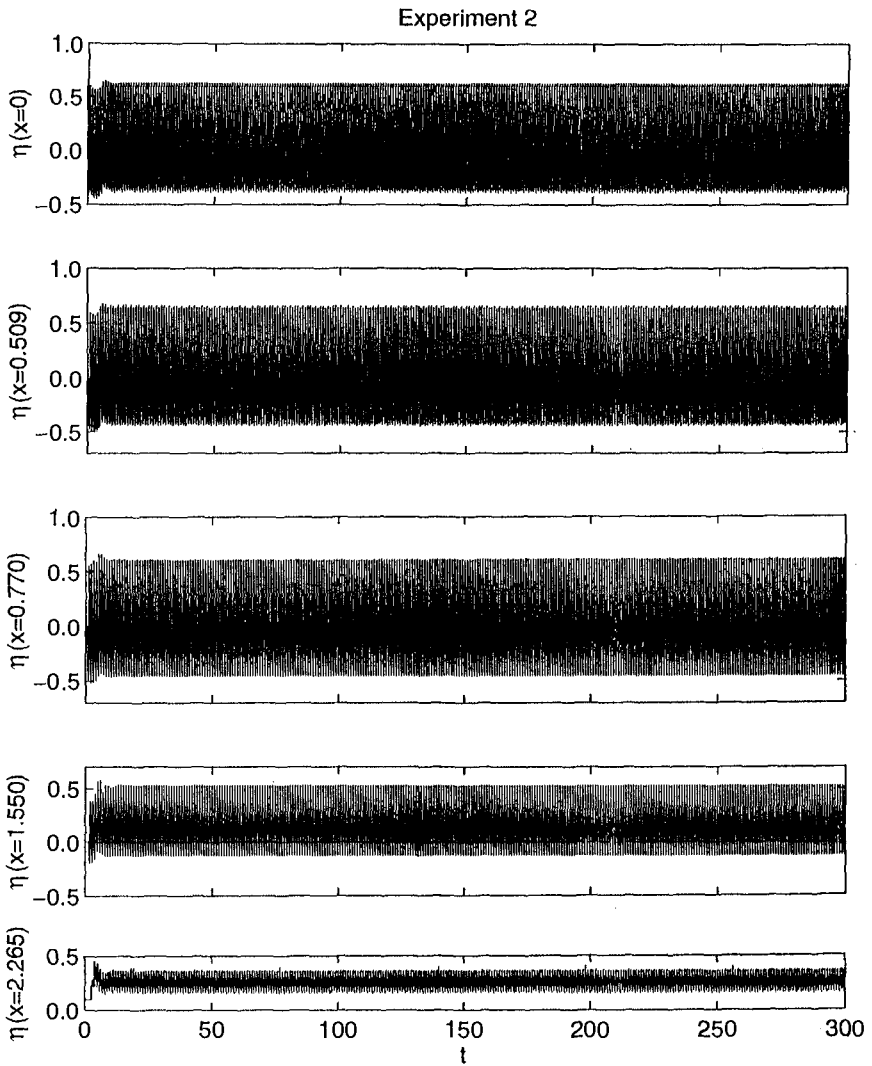


Figure 2: Computed Temporal Variations of Free Surface Elevation η at $x = 0, 0.509, 0.770, 1.550$ and 2.265 .

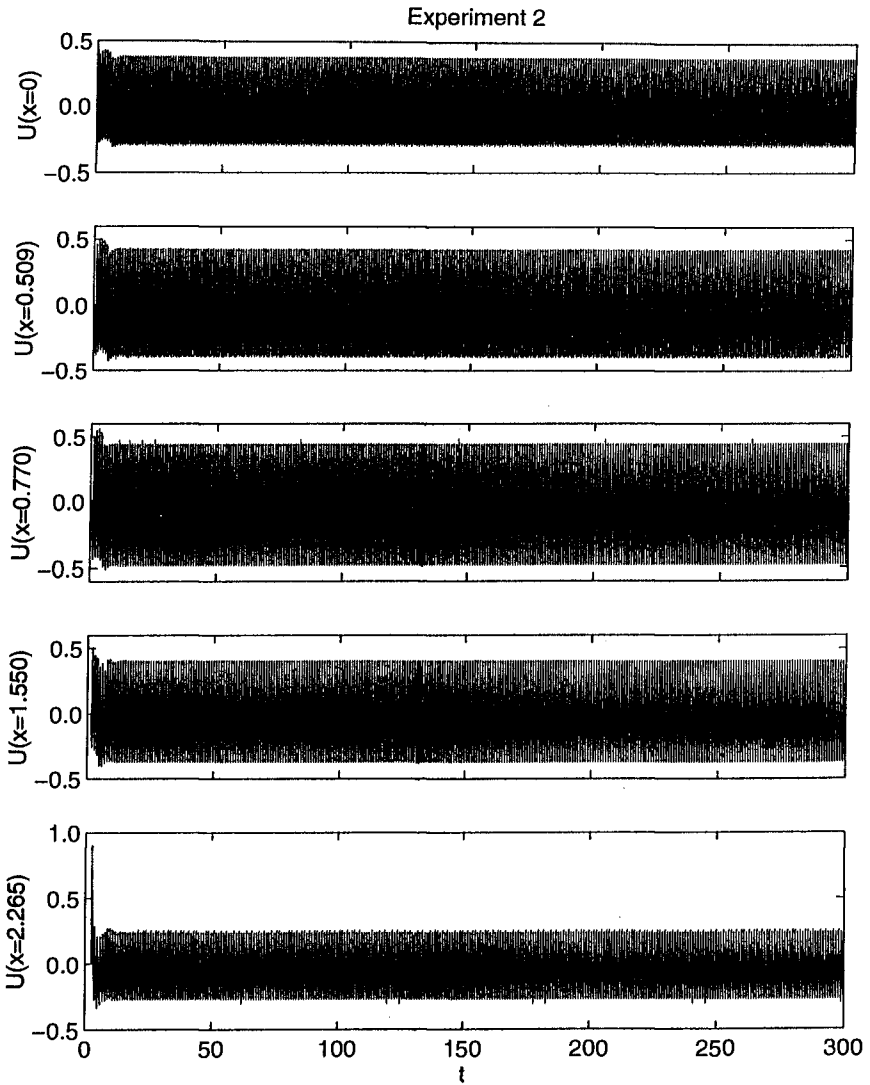


Figure 3: Computed Temporal Variations of Cross-Shore Velocity U at $x = 0, 0.509, 0.770, 1.550$ and 2.265 .

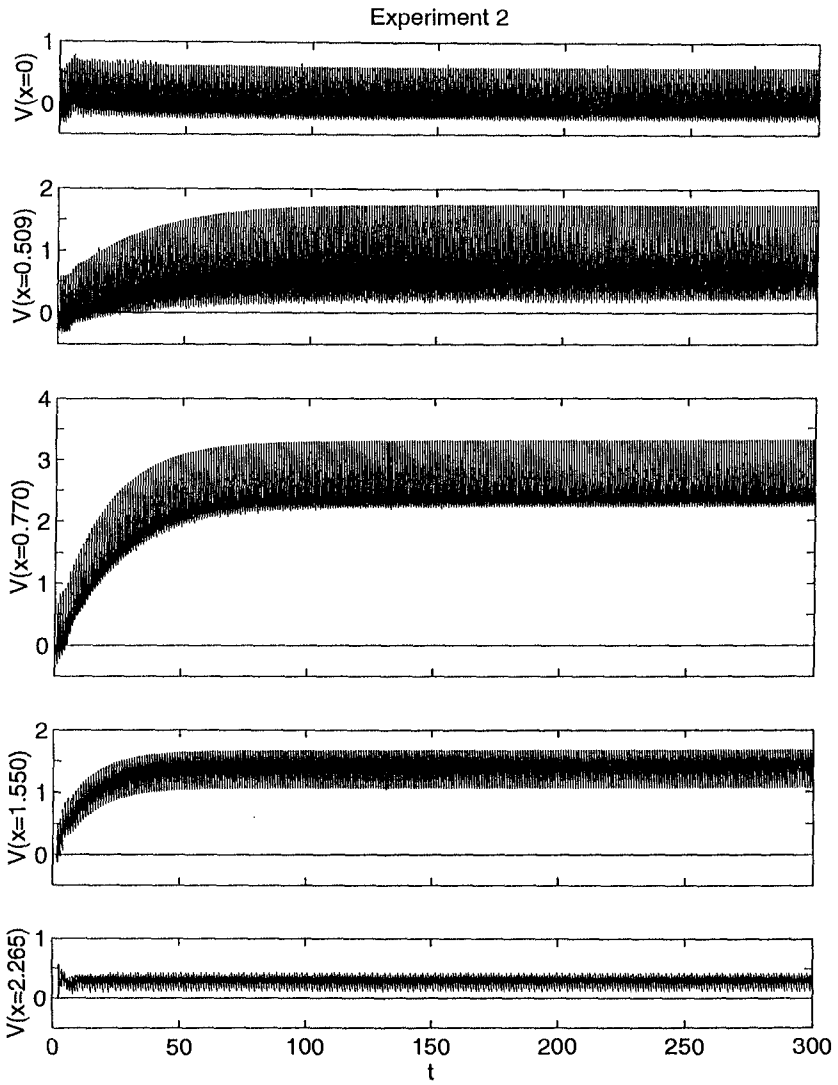


Figure 4: Computed Temporal Variations of Alongshore Velocity V at $x = 0, 0.509, 0.770, 1.550$ and 2.265 .

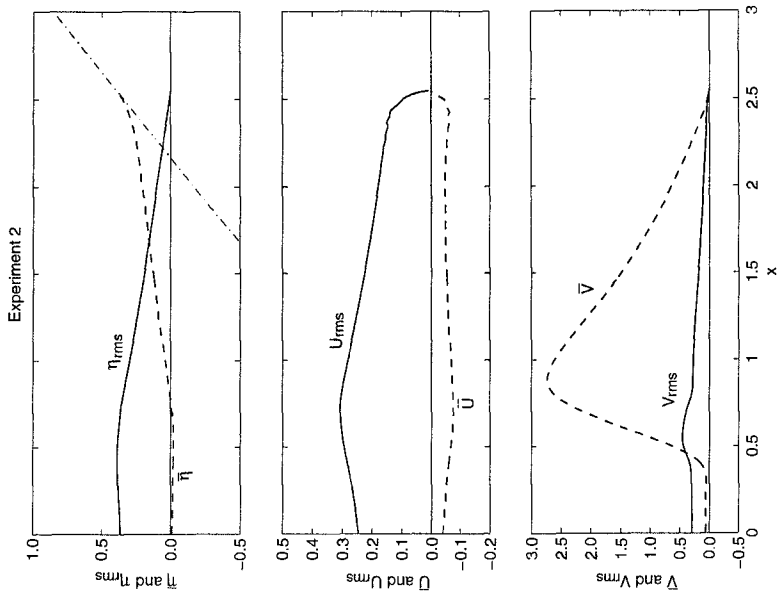


Figure 5: Cross-Shore Variations of $\bar{\eta}$, η_{rms} , \bar{U} , U_{rms} , \bar{V} and V_{rms}

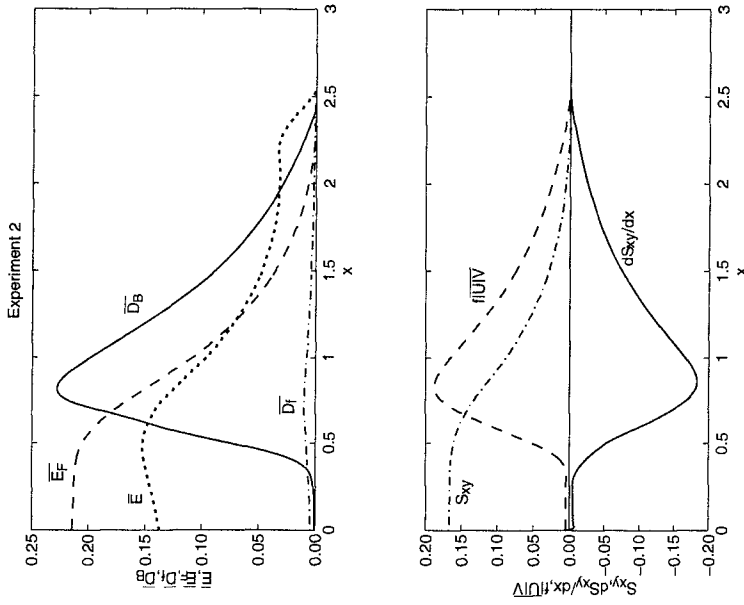


Figure 6: Time-Averaged Cross-Shore Wave Energy and Alongshore Momentum Balances.

volved in the time-averaged cross-shore wave energy equation (Kobayashi and Wurjanto 1992) and the time-averaged alongshore momentum equation (6) where \bar{E} = specific energy per unit horizontal area; \bar{E}_F = energy flux per unit width; \bar{D}_f = energy dissipation rate due to bottom friction per unit horizontal area; \bar{D}_B = energy dissipation rate due to wave breaking per unit horizontal area; S_{xy} = alongshore radiation stress given by (7); and $f|\bar{U}|\bar{V}$ = alongshore bottom shear stress. The top figure in Fig. 6 indicates that the energy dissipation due to wave breaking is dominant and does not occur suddenly in this numerical model which does not account for wave breaking explicitly (Kobayashi and Wurjanto 1992). For these experiments of alongshore uniformity, the computed alongshore gradients of the mean and variance of η are negligible and the time-averaged alongshore momentum equation (6) reduces to $dS_{xy}/dx = -f|\bar{U}|\bar{V}$. The bottom figure in Fig. 6 shows that S_{xy} decreases monotonically in the surf and swash zones. The computed cross-shore variations of dS_{xy}/dx and $-f|\bar{U}|\bar{V}$ are essentially the same where $f|\bar{U}|\bar{V}$ is plotted to distinguish the two curves.

Fig. 7 compares the measured and computed cross-shore variations of the normalized local wave height H for each of the four experiments listed in Table 1. The agreement is very good in view of no adjustable parameter included in this numerical model to initiate wave breaking. However, it should be stated that this numerical model can not predict wave shoaling without wave breaking over a long distance (Kobayashi et al. 1989).

Fig. 8 compares the measured and computed cross-shore variations of the normalized wave setup $\bar{\eta}$ together with the normalized uniform slope indicated by the dotted line for each of the four experiments. The agreement is good in the swash zone but the computed mean water level rises too rapidly landward of the breaker line as was the case with the previous comparison by Kobayashi et al. (1989). The numerical model does not predict the transition zone of constant wave setback whose effects on surf zone hydrodynamics were reviewed and elaborated by Nairn et al. (1990).

Table 2 shows the comparisons of the measured and computed maximum setup and runup for the four experiments. The computed maximum setup and runup correspond to the mean and maximum shoreline elevations, respectively, measured by hypothetical wires placed parallel to the above the uniform slope at elevations of 1, 5 and 10 mm,

Table 2: Measured and Computed Maximum Setup and Runup

Expt. No.	Maximum Setup				Runup			
	Computed			Meas.	Computed			Meas.
	1mm	5mm	10mm		1mm	5mm	10mm	
2	0.34	0.29	0.26	0.29	0.38	0.35	0.35	0.43
3	0.34	0.28	0.25	0.31	0.38	0.35	0.35	0.47
4	0.19	0.17	0.17	0.20	0.20	0.20	0.21	0.24
5	0.28	0.23	0.21	0.27	0.31	0.29	0.29	0.34

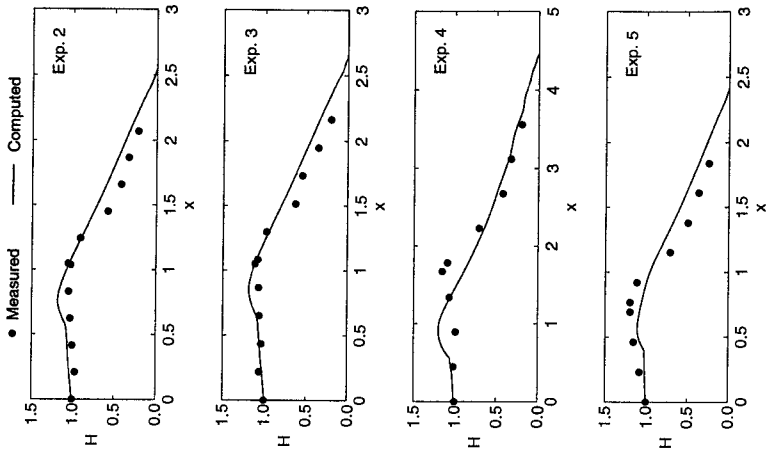


Figure 7: Measured and Computed Local Wave Height H for Four Experiments.

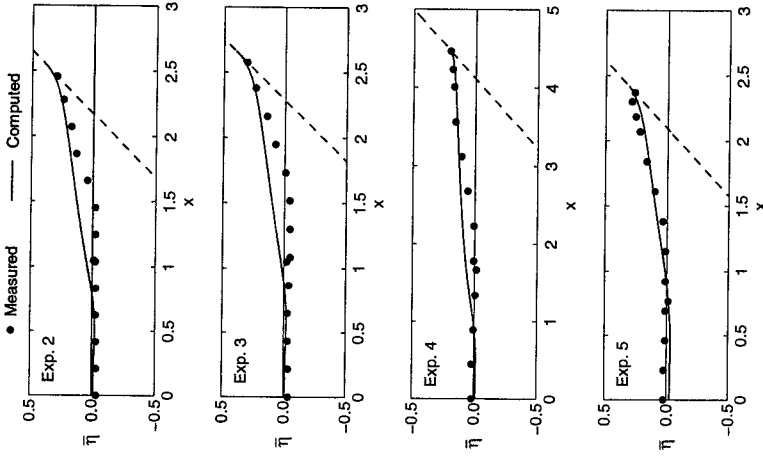


Figure 8: Measured and Computed Wave Setup $\bar{\eta}$ for Four Experiments.

whereas the actual measurements were made visually. The computed results are not very sensitive to the wire elevations and in fair agreement with the measured values except that the numerical model with the bottom friction factor $f' = 0.05$ slightly underpredicts the visually measured runup. It is also noted that the swash oscillations in the regular wave experiments are very narrow in comparison to swash oscillations on natural beaches that tend to be dominated by low-frequency motions (Guza and Thornton 1982; Holman and Sallenger 1985).

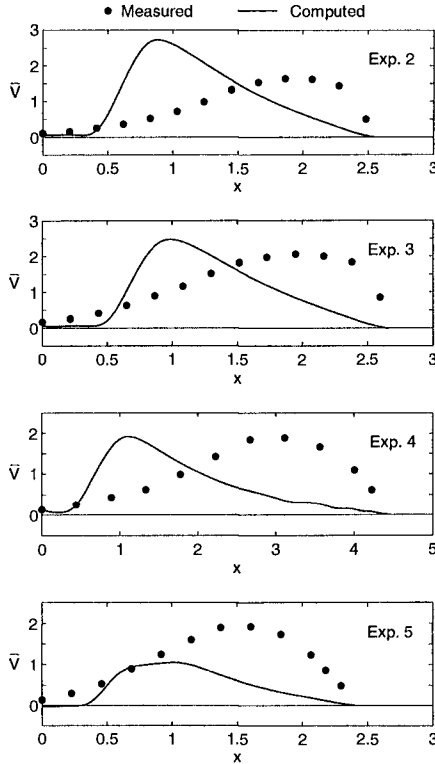


Figure 9: Measured and Computed Longshore Current \bar{V} for Four Experiments.

Finally, Fig. 9 compares the measured and computed cross-shore variations of the longshore current \bar{V} for the four experiments. The numerical model with $f' = 0.05$ predicts the magnitude of \bar{V} but can not predict the shape of \bar{V} probably because the numerical model based on (3) with $C_2 = 1$ does not include lateral mixing (dispersion) and it can not predict the transition zone as shown in Fig. 8. Comparing the similar agreement for Experiments 2 and 3 whose incident wave conditions are listed in Table 1, it may be concluded that $\theta_c^2 = 0.206$ may still be regarded to be much less than unity. Visser (1984) and Nairn et al. (1990) showed it necessary to delay the initiation of the influence of energy dissipation on the generation of longshore currents until the landward limit of the transition zone. These shortcomings of the numerical model

may be serious for longshore currents generated by regular waves but are much less apparent for irregular waves due to irregular wave breaking and generation of low-frequency motions as presented by Kobayashi and Karjadi (1995) who compare the numerical model with available field data on longshore currents (Thornton and Guza 1986).

CONCLUSIONS

A horizontally two-dimensional, time-dependent numerical model is developed for predicting swash and surf hydrodynamics under obliquely incident waves. The assumptions of shallow water waves with small incident angles are made to reduce computational efforts significantly and eliminate difficulties associated with lateral boundary conditions. Under these assumptions, the dominant cross-shore fluid motion along each cross-shore line is computed first using the existing one-dimensional numerical model. The secondary alongshore fluid motion, which may vary slowly in the alongshore direction, is then computed using the computed free surface elevation and cross-shore fluid velocity. The developed numerical model is compared with available data for obliquely incident regular waves. The numerical model is shown to predict the wave height, setup and runup well, although it can not model the transition zone. This implies that the existing one-dimensional model for normally incident waves can be used to predict the cross-shore variations of the free surface elevation for obliquely incident waves with small incident angles. The numerical model with the bottom friction factor calibrated previously for swash oscillations predicts the magnitude of longshore current fairly well but can not reproduce the longshore current profile probably because it does not include the transition zone and lateral mixing. The utility of the developed time-dependent model in comparison to conventional time-averaged models with several adjustable parameters (e.g., Nairn et al. 1990) is not apparent for the compared regular wave data for which the swash zone is narrow and the oscillatory alongshore velocity is small relative to the longshore current.

ACKNOWLEDGEMENTS

This work was supported by the U.S. Army Research Office, University Research Initiative, under Contract No. DAAL03-92-G-0116 and by the NOAA Office of Sea Grant, Department of Commerce, under Grant No. NA85AA-D-SG033 (SG95 R/OE-18).

REFERENCES

- Bodge, K. R., and Dean, R. G. (1987). "Short-term impoundment of longshore transport." *Proc. Coastal Sediment '87*, ASCE, 1,468-483.
- Clausner, J. E., Gebert, J. A., Rambo, A. T., and Watson, K. D. (1991). "Sand bypassing at Indian River Inlet, Delaware." *Proc. Coastal Sediments '91*, ASCE, 1,1177-1191.
- Gharangik, A. M., and Chaudhry, M. H. (1991). "Numerical simulation of hydraulic jump." *J. Hydraulic Eng.*, ASCE, 117(9),1195-1211.
- Guza, R. T., and Thornton, E. B. (1982). "Swash oscillations on a natural beach." *J. Geophys. Res.*, 87(C1),483-491.

- Holman, R. A., and Sallenger, Jr., A. H. (1985). "Setup and swash on a natural beach." *J. Geophys. Res.*, 90(C1),945-953.
- Kamphuis, J. W. (1991). "Alongshore sediment transport rate." *J. Wtrwy. Port Coast. Oc. Eng.*, ASCE, 117(6),624-640.
- Kobayashi, N., DeSilva, G. S., and Watson, K. D. (1989). "Wave transformation and swash oscillation on gentle and steep slopes." *J. Geophys. Res.*, 94(C1),951-966.
- Kobayashi, N., and Karjadi, E. A. (1995). "Obliquely incident irregular waves in surf and swash zones." Submitted to *J. Geophys. Res.*
- Kobayashi, N., Otta, A. K., and Roy, I. (1987). "Wave reflection and runup on rough slopes." *J. Wtrwy. Port Coast. Oc. Eng.*, ASCE, 113(3),282-298.
- Kobayashi, N., and Poff, M. T. (1994). "Numerical model RBREAK2 for random waves on impermeable coastal structures and beaches." *Res. Rpt. No. CACR-94-12*, Ctr. for Applied Coastal Res., Univ. of Delaware, Newark, Del.
- Kobayashi, N., and Wurjanto, A. (1992). "Irregular wave setup and run-up on beaches." *J. Wtrwy. Port Coast. Oc. Eng.*, ASCE, 118(4),368-386.
- MacCormack, R. W. (1969). "The effect of viscosity in hypervelocity impact cratering." *Pap. 69-354*, Am. Inst. Aeronaut. and Astronaut., New York, N.Y.
- Nairn, R. B., Roelvink, J. A., and Southgate, H. N. (1990). "Transition zone width and implications for modelling surf zone hydrodynamics." *Proc. 22nd Coastal Eng. Conf.*, ASCE, 1, 68-81.
- Richtmyer, R. D., and Morton, K. W. (1967). *Difference Methods for Initial-Value Problems*. Interscience, N.Y.
- Rodi, W. (1980). *Turbulence Models and Their Application in Hydraulics*. Intl. Assoc. for Hydraul. Res., Delft, The Netherlands.
- Ryrie, S. C. (1983). "Longshore motion generated on beaches by obliquely incident bores." *J. Fluid Mech.*, 129,193-212.
- Svendsen, I. A., and Putrevu, U. (1994). "Nearshore mixing and dispersion." *Proc. Roy. Soc. Lond.*, A(445), 561-576.
- Thornton, E. B., and Guza, R. T. (1986). "Surf zone longshore currents and random waves: field data and models." *J. Phys. Oceanogr.*, 16,1165-1178.
- Visser, P. J. (1984). "Uniform longshort current measurements and calculations." *Proc. 19th Coastal Eng. Conf.*, ASCE, 2, 2192-2207.
- Visser, P. J. (1991). "Laboratory measurements of uniform longshore currents." *Coastal Eng.*, 15,563-593.